Biochimica et Biophysica Acta 1840 (2014) 2060–2069

Contents lists available at ScienceDirect

Biochimica et Biophysica Acta

journal homepage: www.elsevier.com/locate/bbagen

GATA-4 induces changes in electrophysiological properties of rat mesenchymal stem cells

Hong-Xia Li, Ya-Feng Zhou, Bin Jiang, Xin Zhao, Ting-Bo Jiang, Xun Li, Xiang-Jun Yang *, Wen-Ping Jiang

Department of Cardiology, The First Affiliated Hospital of Soochow University, Suzhou, Jiangsu 215006, China

ARTICLE INFO

Article history:
Received 8 December 2013
Received in revised form 14 February 2014
Accepted 19 February 2014
Available online 26 February 2014

Keywords:
GATA-4
Mesenchymal stem cell
Ion channel
Transdifferentiation
Patch clamp
Electrophysiological property

ABSTRACT

Background: Transplanted mesenchymal stem cells (MSC) can differentiate into cardiac cells that have the potential to contribute to heart repair following ischemic injury. Overexpression of GATA-4 can significantly increase differentiation of MSC into cardiomyocytes (CM). However, the specific impact of GATA-4 overexpression on the electrophysiological properties of MSC-derived CM has not been well documented.
Methods: Adult rat bone marrow MSC were retrovirally transduced with GATA-4 ($MSC^{GATA\text{-}4}$) and GFP (MSC^{Null}) and subsequently co-cultured with neonatal rat ventricular cardiomyocytes (CM). Electrophysiological properties and mRNA levels of ion channels were assessed in MSC using patch-clamp technology and real-time PCR.
Results: $MSC^{GATA\text{-}4}$ exhibited higher levels of the TTX-sensitive Na^+ current ($I_{Na.TTX}$), L-type calcium current ($I_{Ca.L}$), transient outward K^+ current (I_{to}), delayed rectifier K^+ current (IK_{DR}) and inwardly rectifying K^+ current (I_{K1}) channel activities reflective of electrophysiological characteristics of CM. Real-time PCR analyses showed that $MSC^{GATA\text{-}4}$ exhibited upregulated mRNA levels of Kv1.2, Kv2.1, SCN2a1, CCHL2a, KV1.4 and Kir1.1 channels versus MSC^{Null}. Interestingly, $MSC^{GATA\text{-}4}$ treated with IGF-1 neutralizing antibodies resulted in a significant decrease in Kir1.1, Kv2.1, KV1.4, CCHL2a and SCN2a1 channel mRNA expression. Similarly, $MSC^{GATA\text{-}4}$ treated with VEGF neutralizing antibodies also resulted in an attenuated expression of Kv2.1, Kv1.2, Kv1.4, Kir1.1, CCHL2a and SCN2a1 channel mRNAs.
Conclusions: GATA-4 overexpression increases I_{to}, IK_{DR}, I_{K1}, $I_{Na.TTX}$ and $I_{Ca.L}$ currents in MSC. Cytokine (VGEF and IGF-1) release from GATA-4 overexpressing MSC can partially account for the upregulated ion channel mRNA expression.
General significance: Our results highlight the ability of GATA4 to boost the cardiac electrophysiological potential of MSC.

1. Introduction

Transplantation of bone marrow mesenchymal stem cells (MSC) has been shown to play an increasingly prevalent therapeutic role in the treatment of many heart diseases, such as myocardial infarction and cardiac hypertrophy [1,2]. MSC transplantation has been shown to improve the cardiac function of injured hearts [3,4] through the regeneration of cardiomyocytes (CM) [5,6] as well as paracrine effects that promote angiogenesis, decrease cardiac fibrosis, and prevent host cardiomyocyte apoptosis [7]. It has been reported that genetic engineering of MSC represents a useful strategy for boosting the therapeutic potency of MSC [8,9].

GATA-4 is a member of the GATA family of zinc finger transcription factors and an early marker of the cardiomyocyte lineage [10,11]. GATA-4 has multiple important roles in promoting cell survival, cell differentiation, angiogenesis and cardioprotection [11–14]. GATA-4 is also a critical factor for differentiation of pluripotent (P19) stem cells into beating CM [15]. We have previously reported that overexpression of GATA-4 in MSC ($MSC^{GATA\text{-}4}$) significantly increases MSC survival in ischemic myocardium and that treatment of animals with myocardial infarction with $MSC^{GATA\text{-}4}$ can significantly improve their cardiac function as assessed by echocardiography [13]. Recently, we also demonstrated that overexpression of GATA-4 significantly promotes the differentiation of MSC into CM, by assessing for CM specific markers using quantitative real-time polymerase chain reaction (real-time PCR) and Western blot analyses [16].

Transplantation of $MSC^{GATA\text{-}4}$ can effectively improve cardiac function in the setting of myocardial infarction as well as directly promote their differentiation into CM; however, the impact of GATA-4 overexpression on the electrophysiological properties of MSC remains unclear. Since the transient outward K^+ current (I_{to}), inwardly rectifying K^+ current (I_{K1}), TTX-sensitive Na^+ current ($I_{Na.TTX}$) and L-type calcium

Abbreviations: CM, cardiomyocytes; MSC, mesenchymal stem cells; MSC^{Null}, MSC transduced only with EGFP; $MSC^{GATA\text{-}4}$, MSC transduced with GATA-4 and EGFP; I_{K1}, inward rectifier K^+ current; IK_{DR}, delayed rectifier K^+ current; I_{to}, transient outward K^+ current; $I_{Na.TTX}$, TTX-sensitive Na^+ current; $I_{Ca.L}$, L-type calcium current; CCHL2a, L-type calcium channel α-2 subunit; GAPDH, glyceraldehyde-3-phosphate dehydrogenase; Kir, inward rectifier potassium channel; Kv, voltage-gated potassium channel

* Corresponding author. Tel.: +86 512 67781225; fax: +86 512 67781712.
E-mail address: yxjdemail@126.com (X.-J. Yang).

http://dx.doi.org/10.1016/j.bbagen.2014.02.020
0304-4165/

current ($I_{Ca.L}$) are highly expressed in CM and contribute to the electrophysiological actions of CM [17–21], we hypothesized that GATA-4 overexpression would upregulate these functional ion channels (I_{to}, I_{K1}, $I_{Na.TTX}$ and $I_{Ca.L}$) within $MSC^{GATA\text{-}4}$ to promote their differentiation to CM. The present study was designed to investigate the effects of GATA-4 on the electrophysiological properties of MSC as well as uncover potential regulatory mechanisms.

2. Material and methods

All protocols conform to the *Guidelines for the Care and Use of Laboratory Animals* prepared by the National Academy of Sciences and published by the National Institutes of Health (NIH Publication No. 85-23, revised 1996). All animal procedures were in full compliance with the guidelines approved by the University of Soochow Animal Care and Use Committee.

2.1. MSC culture

MSC were obtained from femurs and tibias of Sprague–Dawley rats, as previously described [22]. Cells were cultured in Iscove's Modified Dulbecco's Medium (IMDM) supplemented with 10% FBS, 100 U/ml penicillin and 100 μg/ml streptomycin at 37 °C in humid air with 5% CO_2. After being seeded for two days, MSC adhered to the bottom of culture plates, while hematopoietic cells remained suspended in the medium. The culture medium was changed every three days and the non-adherent hematopoietic cells were completely washed out after four changes of media.

2.2. MSC retroviral transduction with GATA-4 and GFP plasmids

MSC from the second passage were used to overexpress recombinant GATA-4. A retrovirus expressing full-length GATA-4 cDNA was constructed using the pMSCV retroviral expression system (Clontech, America). GP2-293 cells (Clontech, America) were co-transfected with either pMSCV-GATA-4-IRES-EGFP and pVSVG or pMSCV-IRES-EGFP and pVSVG for generation of $MSC^{GATA\text{-}4}$ and MSC^{Null}, respectively. After 48 h, supernatants were filtered and incubated with MSC in the presence of 10 μg/ml polybrene (Sigma) for 12 h. Stable clones for $MSC^{GATA\text{-}4}$ and MSC^{Null} were obtained by puromycin selection (Sigma; 3 μg/ml for 5 days) and verified for construct integration by quantitative real-time PCR and Western blot analyses.

2.3. Quantitative real-time PCR

Total RNA was isolated from MSC using TRIzol (Invitrogen) as per the manufacturer's instructions and further treated with DNase I (Invitrogen). Quantitative real-time PCR to detect ion channels was carried out on an iQ5 real-time system using an iQ SYBR Super-mix (Bio-Rad, Hercules, CA, USA) as described previously [23]. Briefly, complementary DNA was synthesized using SuperScript™ III First-Strand Synthesis for real-time PCR (Invitrogen). The cDNAs were subsequently amplified using Taq DNA polymerase in the presence of specific primers for each ion channel (Table 1) under the following conditions: the mixture was annealed at 50–60 °C (1 min), extended at 72 °C (2 min), and denatured at 95 °C (45 s) for 35 to 40 cycles. This was followed by a final extension at 72 °C (10 min) to ensure complete product extension. Target mRNA expression relative to glyceraldehyde-3-phosphate dehydrogenase (GAPDH) was calculated based on the threshold cycle (C_T) as $r = 2^{-\Delta\ (\Delta C_T)}$, where $\Delta C_T = C_{T\ target} - C_{T\ GAPDH}$ and $\Delta(\Delta C_T) = \Delta C_{T\ experimental} - \Delta C_{T\ control}$.

2.4. Immunoblotting

Cells were washed in phosphate-buffered saline (PBS) and homogenized in a lysis buffer. Nuclear proteins were extracted using a NE-PER® Nuclear and Cytoplasmic Extraction Reagent (Thermo Scientific Co.) according to the supplier's instructions. Protein concentrations were quantified using a Bio-Rad DC-Protein Assay Reagent (Bio-Rad). Denatured proteins (25 μg) were separated by SDS-PAGE using 12% gels, transferred to nitrocellulose membrane (Bio-Rad), and immunoblotted overnight at 4 °C with primary antibodies to GATA-4 (Abcam). Membranes were then incubated for 1 h with a HRP-conjugated secondary antibody at room temperature, washed and developed with the ECL plus kit (GE Healthcare, USA). Blots were analyzed by densitometry with NIH image software (AlphaEase FC, Version 6.0.0).

2.5. Cardiomyocyte isolation and co-culture with MSC

Ventricular CM were isolated from neonatal (1–3 days old) Sprague–Dawley rat ventricles, using a neonatal CM isolation kit (Worthington Biochemical Co.) in accordance with the supplier's instructions. CM were identified by immunostaining cells with anti-α-sarcomeric actinin antibody (clone EA-53; Sigma).

$MSC^{GATA\text{-}4}$ and neonatal ventricular CM were co-cultured at a ratio of 1:10 in a dual-set system in which CM and MSC shared the same medium but were separated by a semi-permeable membrane (Corning). In this dual-set culture system, CM were seeded in the upper layer and MSC were seeded in the lower layer. For controls, MSC^{Null} were co-cultured with CM. After two weeks of co-culture, MSC were immunostained for cardiac troponin T using specific antibodies (cTnT, Santa Cruz Biotech). All studies were performed in triplicate using samples from independent culture preparations. The percentage of cTnT staining cells was determined from an analysis of over 1000 DAPI-positive cells. The electrophysiological properties of ion channels in $MSC^{GATA\text{-}4}$ and MSC^{Null} after being co-cultured with CM were assessed by patch-clamp technology and real-time PCR.

2.6. Electrophysiology

$MSC^{GATA\text{-}4}$ and MSC^{Null} were examined by whole-cell patch-clamp techniques [22], after 2 weeks of co-culturing conditions. To record ion channel currents, detached MSC were suspended in a culture medium, transferred to a cell chamber for 15–20 min, allowed to attach to the bottom of the cell chamber, and subsequently superfused with normal

Table 1
Primers used in the analysis of GATA-4 and ion channel genes.

Gene target	GenBank accession no	Forward primer sequence (5′–3′) (sense)	Reverse primer sequence (5′–3′) (antisense)	PCR product (bp)
GATA-4	AB075549.1	CTGTCATCTCACTATGGGCA	CCAAGTCCGAGCAGGAATTT	256
GAPDH	NM_017008	GTGCTGAGTATGTCGTGGAG	GTCTTCTGAGTGGCAGTGAT	301
CCHL2a	M86621	CTCTGAGATGTTAGAAACCCTT	CTTCTCCTCCATCCGTGA	272
Kv2.1a	NM_013186	GCTGCAGAGCCTAGACGAGT	TGCTTTTGAACTTGGTGTCG	452
Kv1.2a	NM_012970	GAGATGTTTCGGGAGGATGA	CTCTGTCCCCAGGGTGATAA	450
Kv4.2	NM_031730	CATGGCCCTGGTGTTCTACT	GCAAGAAGCCCAGTTCTGAC	437
rScn2a1	NM_012647	GCCCAAATACGAAGACAA	AAATAATAATGGCGGAGG	450
Kv1.4a	NM_012971	AGTCAGTTGCCCATACCT	TCCTCGGGACCACCTTTA	495
Kir1.1	NM_017023	CAGACAACGTCGAACAAG	AACCTGAATCCGTAACCT	485

Tyrode's solution containing (in mM): 136 NaCl, 5.4 KCl, 1.0 $MgCl_2$, 1.8 $CaCl_2$, 0.33 NaH_2PO_4, 10 glucose, and 10 4-(2-hydroxyethyl) piperazine-1-ethanesulfonic acid (Hepes); pH adjusted to 7.4 with NaOH at a constant rate of 1.2 ml/min. Borosilicate glass electrodes (1.6 mm OD) were pulled with a Brown-Flaming puller (Model P-97, Sutter Instrument Co.) and had tip resistances of 3–5 MΩ when filled with pipette solution containing (in mM): 20 KCl, 110 K-aspartate, 1.0 $MgCl_2$, 10 Hepes, 0.05 EGTA, 0.1 GTP, 5.0 Na_2-phosphocreatine, and 5.0 Mg_2-ATP; pH adjusted to 7.2 with KOH. The tip potentials were calibrated before the pipette touched the cell. After a gigaohm-seal was obtained by negative suction, the cell membrane was ruptured by gentle suction to establish whole-cell configuration. Membrane currents were low-pass filtered at 2 kHz. The experiments were conducted at room temperature (21–22 °C). Data was acquired with an Axopatch 200B amplifier (Axon, America).

2.7. Adult rat ventricular cardiomyocyte isolation

Healthy adult Sprague–Dawley rats (18 months old) of both sexes were provided by the Experimental Animal Center of Soochow University (Suzhou, China) for isolation studies. Briefly, rats were anesthetized with pentobarbital sodium intraperitoneally (i.p., 30 mg/kg). Hearts were rapidly removed, weighed and cannulated via the aorta for retrograde perfusion using enzymatic solutions as previously described [23]. Following perfusion, the ventricular myocardium was dissected off and transferred into a KB solution containing (in mmol/L): 50 L-glutamic acid, 40 KCl, 20 KH_2PO_4, 20 Taurine, 3 $MgCl_2$, 70 KOH, 0.5 EGTA, 10 HEPES, 10 glucose; pH 7.4 adjusted with KOH. Isolated single ventricular CM were obtained and maintained in KB solution and used within 8 h. Only relaxed, striated, and rod-shaped cells were used for experimental studies, which were conducted at room temperature (21–22 °C).

2.8. Analysis of bFGF, VEGF and IGF-1 levels in MSC culture media

Media from MSC ($MSC^{GATA\text{-}4}$ and MSC^{Null}) co-cultured with CM were switched to serum-free culture media for 24 h. The media were then collected and subjected to centrifugation at 10,000 *g* at 4 °C for 5 min. Supernatants were stored at −20 °C. The concentrations of basic fibroblast growth factor (bFGF), vascular endothelial growth factor (VEGF) and insulin-like growth factor-1 (IGF-1) were measured in supernatants using ELISA kits (R&D Systems) and according to the manufacturer's instructions. For neutralizing antibody studies, IGF-1 and VEGF neutralizing antibodies (Cell Signal, America) were added for 12 h to the media of $MSC^{GATA\text{-}4}$ co-cultured with CM to a final concentration of 4000 ng/ml.

2.9. Statistical analyses

Non-linear curve-fitting software (Origin 7.5) was used to perform curve-fitting procedures. The results are expressed as mean values ± standard error of the mean (SEM). Significance was tested using paired and unpaired Student's t-tests. One-way ANOVA was applied when several groups were compared. A p value < 0.05 was considered statistically significant.

3. Results

3.1. Characterization of rat MSC

We show that isolated primary rat MSC display an elongated and spindle shape closely resembling fibroblasts after 10 days in culture (Fig. 1A), suggesting that MSC could be successfully isolated, purified and expanded from non-adherent cells in vitro.

3.2. Characterization of GATA-4 overexpression in MSC

Retroviral-mediated strategies were utilized to express a GATA-4/GFP bicistronic construct in MSC. Real-time PCR and Western blot analyses demonstrated the successful transduction and expression of a retroviral vector encoding the GATA-4/GFP bicistronic construct. We show that both $MSC^{GATA\text{-}4}$ (expressing GATA-4/GFP bicistronic construct) and MSC^{Null} (expressing GFP bicistronic construct alone) were GFP immunopositive (Fig. 1B). Quantitative real-time PCR analyses indicated that GATA-4 mRNA levels were significantly increased by 267-fold in $MSC^{GATA\text{-}4}$ when compared with MSC^{Null} (Fig. 1C). We further show that $MSC^{GATA\text{-}4}$ also exhibited higher levels of GATA-4 protein when compared with MSC^{Null} (Fig. 1D).

3.3. Characteristics of isolated neonatal rat and adult rat cardiomyocytes

Isolated neonatal rat CM began to beat spontaneously after 24 h in culture. We show that over 95% of CM were immunopositive for α-sarcomeric actinin and display clear sarcomeric organization (Fig. 1E). After co-culturing MSC with CM for 2 weeks, we show that some GATA-4 transduced MSC consistently stain positive for the cardiomyocyte contractile marker, troponin T (cTnT) (Fig. 1F). The percentage of cTnT positive cells was significantly higher in $MSC^{GATA\text{-}4}$ when compared to MSC^{Null} (28.5% ± 2.1% versus 10.1% ± 1.1%, $p < 0.05$), suggesting that GATA-4 expression promotes the differentiation of MSC into CM under co-culturing conditions with CM. We also show that isolated adult rat CM display rod-shaped morphologies (Fig. 1G).

3.4. Electrophysiological properties of MSC

To determine the electrophysiological properties of $MSC^{GATA\text{-}4}$ and MSC^{Null}, we exploited patch-clamp technology to detect functional currents (I_{Na}, $I_{Ca,L}$, I_{K1}, I_{to}, IK_{DR}) found in CM.

3.5. I_{to} in MSC

We show that $MSC^{GATA\text{-}4}$ display properties of I_{to} currents, which are elicited by voltage steps between −60 mV and +70 mV in 10 mV increments from a holding potential of −80 mV (Fig. 2). These effects could be significantly inhibited by 5 mM 4-aminopyridine (4-AP) ($p < 0.05$) and reversed after washout (Fig. 2A) ($p < 0.05$). Specifically, I_{to} was recorded in 50% (8/16) of $MSC^{GATA\text{-}4}$, unlike 25% (4/16) of MSC^{Null}. Representative tracings recorded from MSC^{Null} cells with the same voltage protocol are shown for comparison (Fig. 2B). The average current density of I_{to} (9.34 ± 2.72 pA/pF) in $MSC^{GATA\text{-}4}$ was significantly higher than that of I_{to} in MSC^{Null} (3.21 ± 1.51 pA/pF) at 70 mV (Fig. 2A, B) ($p < 0.05$). It should be noted; however, that the average current densities in MSC were different from adult rat CM (36.06 ± 4.36 pA/pF) at 70 mV (Fig. 2C, D) ($p < 0.05$). Moreover, the average membrane capacitance in $MSC^{GATA\text{-}4}$ (50.21 ± 8.13 pF) was also significantly higher than MSC^{Null} (33.18 ± 7.14 pF) (Fig. 2D) ($p < 0.05$), but much lower than adult rat CM (116.43 ± 9.71 pF) at 70 mV (Fig. 2D) ($p < 0.05$).

3.6. I_{K1} in MSC

We show that $MSC^{GATA\text{-}4}$ display properties of I_{K1} currents, which are activated by voltage steps between −120 mV and 0 mV in 10 mV increments from a holding potential of −40 mV (Fig. 3). These properties are significantly inhibited by 500 μM $BaCl_2$ ($p < 0.05$) and reversed after washout (Fig. 3A) ($p < 0.05$). We show that $MSC^{GATA\text{-}4}$ display a current–voltage relationship (I–V curve), which is highlighted by the absence and presence of 500 μM $BaCl_2$ and that can be reversed after washout (Fig. 3A). Ba^{2+}-sensitive I_{K1} currents exhibit an I–V curve typical of inward rectifying currents. Representative tracings from MSC^{Null} and adult rat CM recorded with the same voltage protocol are shown for comparison (Fig. 3B, C). I_{K1} currents could be recorded in

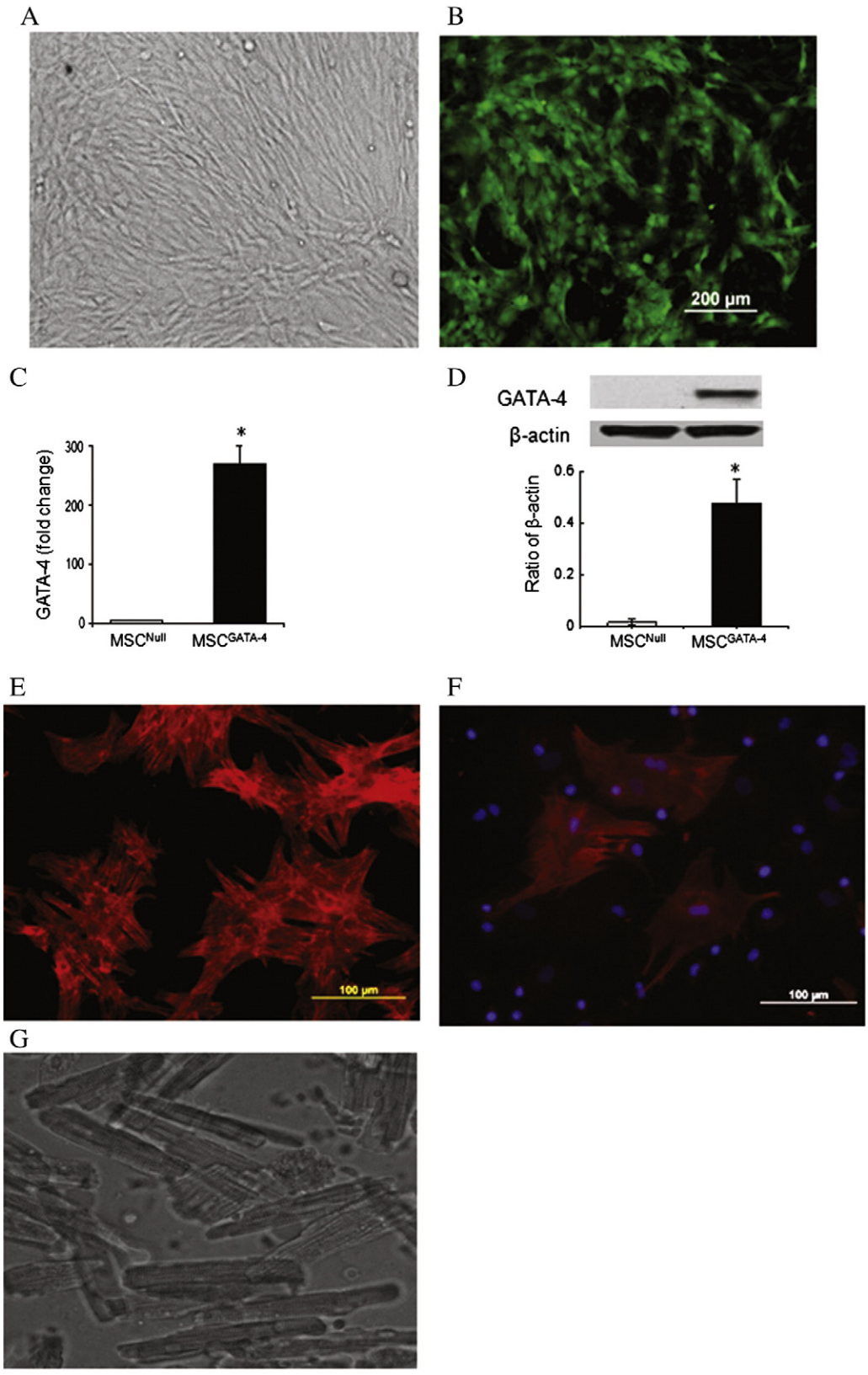

Fig. 1. Characterization of cultured MSC, neonatal and adult rat CM as well as MSC expressing GATA-4 ($MSC^{GATA\text{-}4}$) and empty vector (MSC^{Null}). (A) Cultured primary MSC (10 days) reached confluence with a consistent and homogeneous morphology (magnification = 150×). (B) $MSC^{GATA\text{-}4}$ are GFP-positive. (C) Quantitative real-time PCR analyses of GATA-4 expression. $^{*}p < 0.05$ vs MSC^{Null} group, n = 6. (D) Western blot analysis of GATA-4 protein and corresponding semi-quantitative analysis of data. $^{*}p < 0.05$ vs MSC^{Null}, n = 6. (E) Primary cultured neonatal rat CM (5 days) were stained with anti-α-sarcomeric actinin (α-SA) antibody. CM were positive for α-SA (red) and demonstrate a clear sarcomeric organization. (F) Representative $MSC^{GATA\text{-}4}$ co-cultured with CM, which is stained positive for cardiac troponin T. Nuclei were counterstained with DAPI. (G) Morphology of adult rat CM (magnification = 100×).

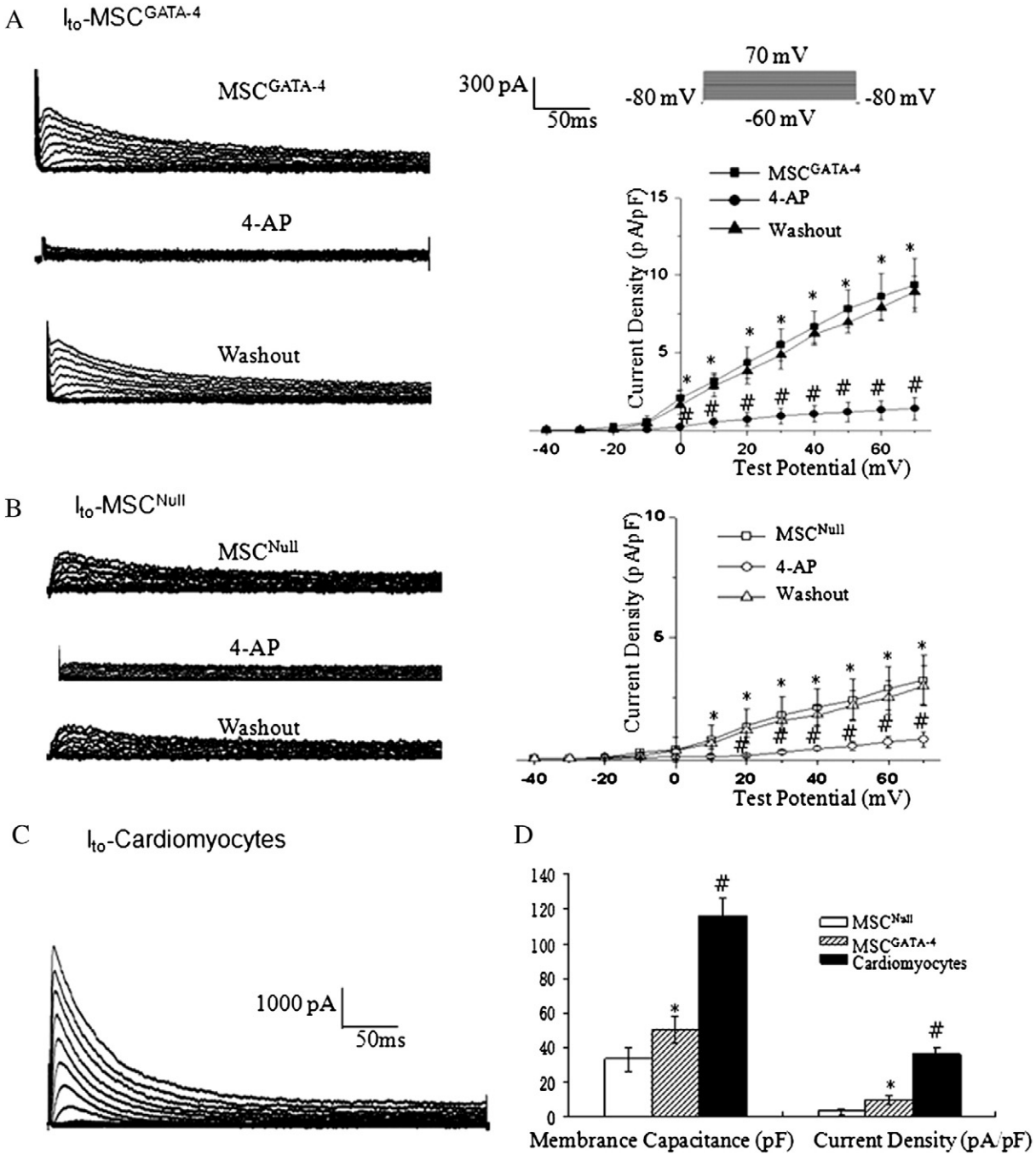

Fig. 2. Functional analysis of transient outward K^+ current (I_{to}) in MSC^{GATA-4}, MSC^{Null} and adult rat CM. (A) Representative traces of I_{to} recorded in MSC^{GATA-4} with a voltage step protocol as shown in the inset in the absence and presence of 5 mM 4-AP. The I–V curve was shown in the absence and presence of 5 mM 4-AP. n = 8. I_{to} was significantly suppressed by 4-AP ($^{\#}p < 0.05$ at 0 to 70 mV vs MSC^{GATA-4} group) and the effect was reversed after drug washout ($^{*}p > 0.05$ vs MSC^{GATA-4} group). (B) Representative traces of I_{to} recorded from MSC^{Null} with the same voltage step protocol in the absence and presence of 5 mM 4-AP. The I–V curve is shown in the absence and presence of 5 mM 4-AP, n = 4. I_{to} was significantly suppressed by 4-AP ($^{\#}p < 0.05$ at 10 to 70 mV vs MSC^{Null} group) and the effect was reversed after drug washout ($^{*}p > 0.05$ vs MSC^{Null} group). (C) Representative traces of I_{to} recorded in adult rat ventricular CM with the same voltage step protocol used in MSC. (D) Comparison of membrane capacitance and I_{to} current densities in MSC^{Null} (n = 4), MSC^{GATA-4} (n = 8) and adult rat ventricular CM (n = 8) at 70 mV ($^{*}p < 0.05$ vs MSC^{Null}. $^{\#}p < 0.05$ vs MSC^{GATA-4}).

60% (18/30) of MSC^{GATA-4}, as compared to 20% (6/30) in MSC^{Null}. Furthermore, the average current density of I_{K1} was increased in MSC^{GATA-4} versus MSC^{Null} (-15.53 ± 4.09 pA/pF versus -6.61 ± 3.72 pA/pF) at -120 mV ($p < 0.05$), but significantly different from adult rat CM (-30.06 ± 5.88 pA/pF) at -120 mV (Fig. 3D) ($p < 0.05$).

3.7. IK_{DR} in MSC

We show that MSC^{GATA-4} also display properties of outward delayed rectifier currents, IK_{DR}, which are elicited by voltage steps between -60 mV and 70 mV in 10 mV increments from a holding potential of -80 mV and then back to -30 mV (Fig. 4). We observed IK_{DR} currents in 54.54% (6/11) of MSC^{GATA-4} and 36.36% (4/11) of MSC^{Null}. Fig. 4A displays representative IK_{DR} traces from MSC^{GATA-4} and MSC^{Null}, which could be significantly inhibited by 5 mM tetraethylammonium (TEA) (Fig. 4B). We also show that these effects could be reversed after drug washout (Fig. 4C). The average step current density of IK_{DR} in MSC^{GATA-4} (13.1 ± 2.3 pA/pF) was significantly higher than MSC^{Null} (8.8 ± 1.8 pA/pF) at $+70$ mV ($p < 0.05$).

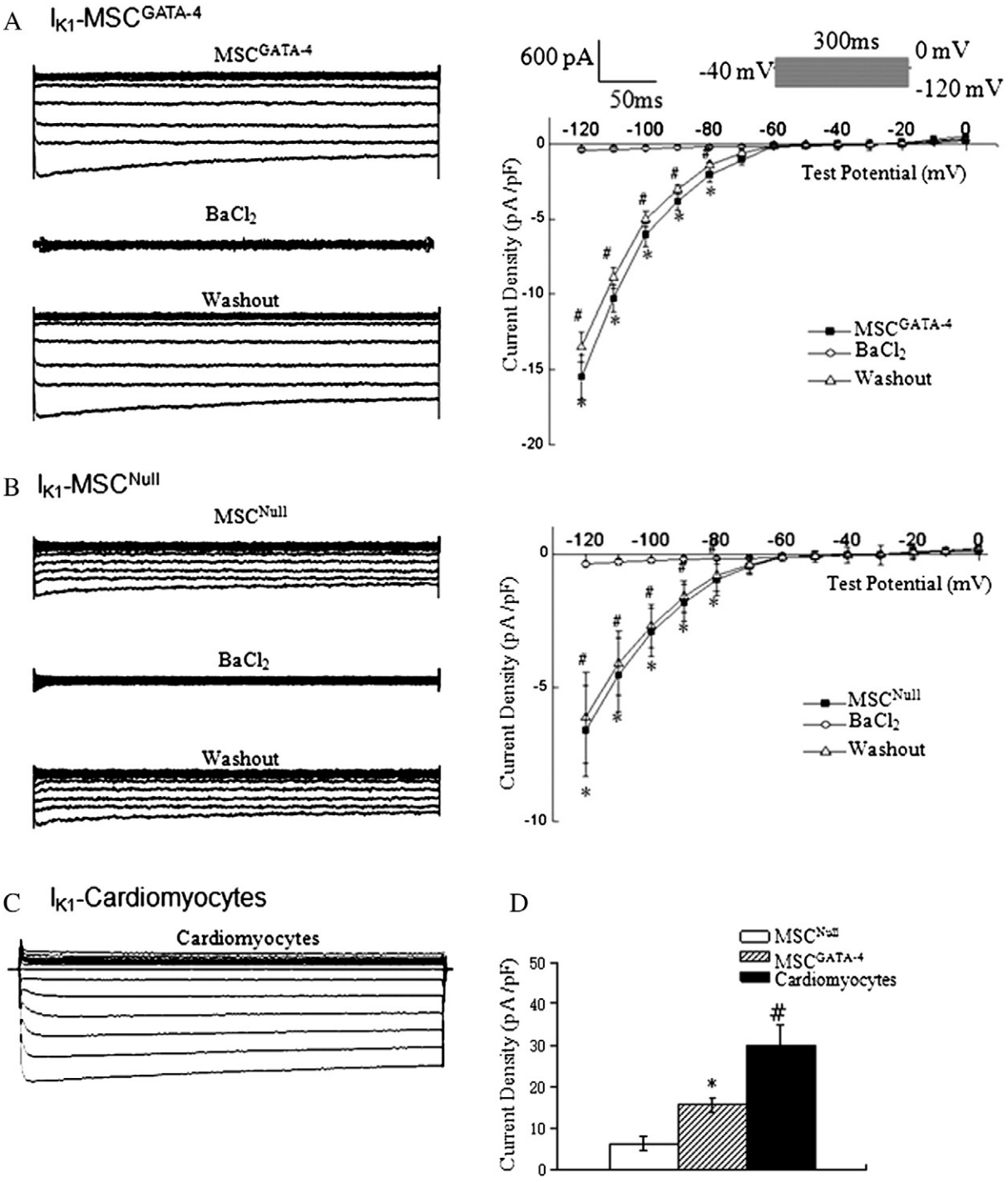

Fig. 3. Functional analysis of I_{K1} in MSC^{GATA-4}, MSC^{Null} and adult rat ventricular CM. (A) Representative traces of I_{K1} recorded in MSC^{GATA-4} in the absence and presence of 500 μM $BaCl_2$. The current was elicited with 300 ms voltage steps from −40 to between −120 and 0 mV as shown in the inset. The I–V curve was shown in the absence (■) and presence (○) of 500 μM $BaCl_2$ as well as the current (Δ) obtained after washout. Ba^{2+} significantly inhibited I_{K1} at −120 to −80 mV. $^{*}p < 0.05$ vs $BaCl_2$ group. $^{\#}p < 0.05$ vs $BaCl_2$ group, n = 10. (B) Representative tracings of I_{K1} recorded in MSC^{Null} in the absence and presence of 500 μM $BaCl_2$ with the same protocol. The I–V curve was shown in the absence (■) and presence (○) of 500 μM $BaCl_2$ as well as the current (Δ) obtained after washout. Ba^{2+} significantly inhibited I_{K1} at −120 to −80 mV. $^{*}p < 0.05$ vs $BaCl_2$ group and $^{\#}p < 0.05$ vs $BaCl_2$ group, n = 6. (C) Representative traces of I_{K1} in adult rat ventricular CM with the same protocol used in MSC. (D) Analysis of I_{K1} current densities in MSC^{Null}, MSC^{GATA-4} and adult rat ventricular CM. $^{*}p < 0.05$ vs MSC^{Null} and $^{\#}p < 0.05$ vs MSC^{GATA-4}, n = 6.

3.8. I_{Na} in MSC

We also found that 20% (5/25) of MSC^{GATA-4} displayed electrophysiological properties of an inward current, sensitive to inhibition by the I_{Na} blocker tetrodotoxin (TTX; 100 nM) and resistant to inhibition by the $I_{Ca.L}$ blocker nifedipine (10 μM). Fig. 5A illustrates representative traces from MSC^{GATA-4}. Our data highlight that activation of the inward current was followed by a gradual activation of the IK_{DR} current. We show that TTX could abolish the inward current (Fig. 5B) and the effect could be reversed upon drug washout for 5 min (Fig. 5C), suggesting that the inward current may be TTX-sensitive I_{Na}. We also show that the density of $I_{Na.TTX}$ in MSC^{GATA-4} is about −4.51 ± 1.01 pA/pF at

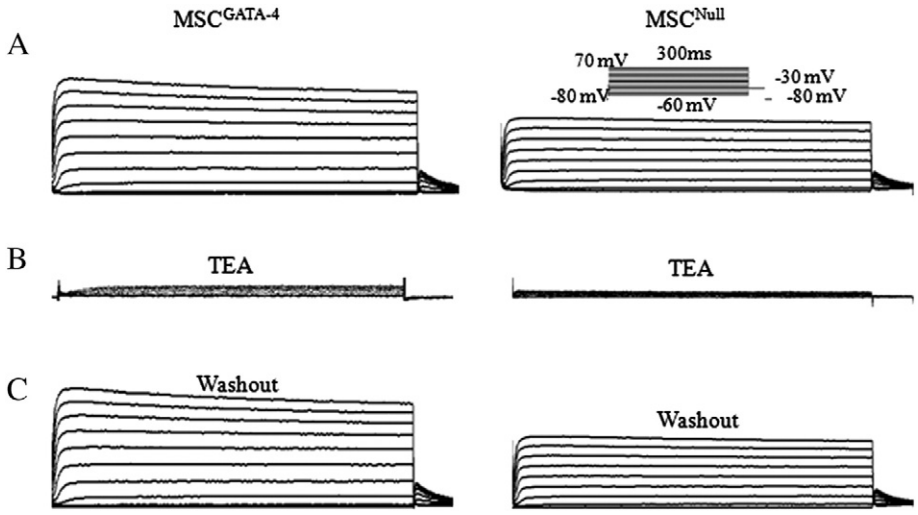

Fig. 4. Functional analysis of delayed rectifier K^+ current (IK_{DR}) in MSC^{GATA-4} and MSC^{Null}. (A) Representative traces of IK_{DR} recorded in MSC^{GATA-4} and MSC^{Null} with the voltage protocol shown in the inset in panel A. (B) Representative traces of IK_{DR} recorded in MSC^{GATA-4} and MSC^{Null} in the presence of 5 mM TEA. (C) Representative traces of IK_{DR} recorded in MSC^{GATA-4} and MSC^{Null} after drug washout. IK_{DR} was reduced by 5 mM TEA and the effect was fully recovered upon washout.

−30 mV, which was found to be significantly lower than adult rat CM (−9.31 ± 0.91 pA/pF) ($p < 0.05$). Interestingly, we could not identify properties of this current in MSC^{Null} (Fig. 5D).

3.9. $I_{Ca.L}$ in MSC

Through the addition of the K^+ current blocker $CsCl_2$ and Na^+ current blocker TTX, we identified another inward current in 12% (3/25) of MSC^{GATA-4}, which was sensitive to inhibition by the $I_{Ca.L}$ blocker nifedipine (10 μM; Fig. 6A). However, this current could not be identified in MSC^{Null} (Fig. 6B), suggesting that nifedipine-sensitive $I_{Ca.L}$ currents are only present in a small population of MSC^{GATA-4}. The density of $I_{Ca.L}$ in MSC^{GATA-4} was about −3.31 ± 0.81 pA/pF at 0 mV; however, this was much lower than that observed in adult rat CM (−5.73 ± 0.84 pA/pF) at 0 mV (Fig. 6C) ($p < 0.05$).

3.10. Expression of bFGF, VEGF and IGF-1 in MSC

In order to determine the growth factors important to maintain MSC^{GATA-4} and elucidate the potential mechanisms regulating GATA-4 effects on ion channel levels in MSC, we measured levels of bFGF, VEGF and IGF-1 in the culture media from MSC by ELISA. We show that both VEGF and IGF-1 levels were significantly increased in the culture media from MSC^{GATA-4} (IGF-1 = 21.5 ± 3.2 ng/ml and VEGF = 24.8 ± 1.8 ng/ml) versus MSC^{Null} (IGF-1 = 4.9 ± 0.9 ng/ml and VEGF = 16.2 ± 1.9 ng/ml) (Fig. 7A) ($p < 0.05$). However, we show that bFGF levels were not significantly altered (MSC^{GATA-4}: 512.5 ± 62.4 ng/ml versus MSC^{Null}: 479.6 ± 48.3 ng/ml, $p > 0.05$) between the two groups (Fig. 7B).

3.11. Messenger RNA expression of ion channels in MSC

Rat MSC express several ion channels that play important roles in generating I_{K1}, I_{to} and I_{Na} currents as well as several other currents [16]. Here, we investigated whether GATA-4 would influence the expression of mRNAs of selected ion channels found in CM. To this end, we show that mRNA levels of Kv1.4 and Kv4.2 (likely responsible for I_{to}), Kv1.2 and Kv2.1 (likely responsible for I_{KDR}), SCN2a1 (likely responsible for $I_{Na.TTX}$), Kir1.1 (likely responsible for I_{K1}) and CCHL2a (likely responsible for $I_{Ca.L}$) could be detected in MSC^{GATA-4} and MSC^{Null} using

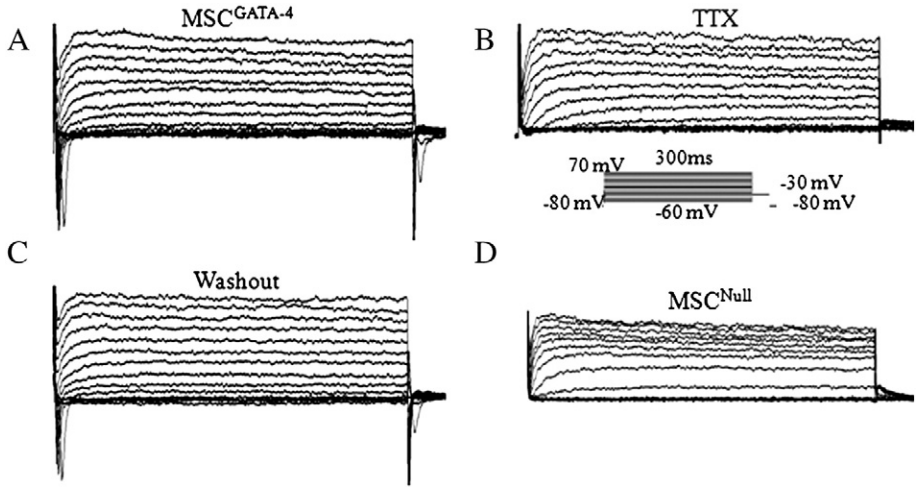

Fig. 5. Functional analysis of I_{Na} in MSC^{GATA-4} and MSC^{Null}. (A) Representative traces of I_{Na} in MSC^{GATA-4} utilizing the voltage protocol as shown in the inset. (B) Representative traces were recorded after the application of 100 nM TTX for 5 min. (C) Representative traces were recorded after drug washout for 5 min. TTX reversibly abolished the inward transient without affecting the outward current, suggesting that the inward current is a TTX-sensitive Na^+ current ($I_{Na.TTX}$). (D) Representative tracings of currents in MSC^{Null} utilizing the voltage protocol as shown. $I_{Na.TTX}$ were not present in MSC^{Null}.

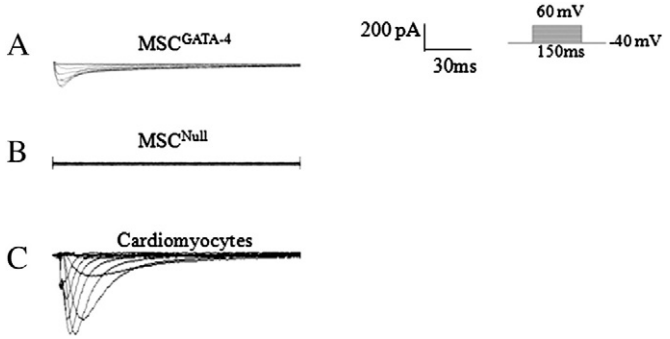

Fig. 6. Functional analysis of $I_{Ca.L}$ in MSC^{GATA-4}, MSC^{Null} and adult rat ventricular CM. (A) Representative traces of $I_{Ca.L}$ in MSC^{GATA-4} utilizing the voltage protocol as shown in the inset. (B) Representative tracings of current in MSC^{Null} utilizing the same voltage protocol. $I_{Ca.L}$ was not present in MSC^{Null}. (C) Representative $I_{Ca.L}$ tracings in adult rat ventricular CM utilizing the same voltage protocol as in MSC.

real-time PCR. The levels of specific mRNAs for these selected ion channels relative to the housekeeping gene GAPDH are summarized in Fig. 8.

The mRNA expression of Kv1.4 channel represented as the ratios of Kv1.4 to GAPDH was significantly increased in MSC^{GATA-4} compared with MSC^{Null} (56.1 ± 7.1% versus 29.1 ± 5.1%, $p < 0.05$) (Fig. 8A). Expression of Kv1.2, Kv2.1, SCN2a1, CCHL2a and Kir1.1 mRNA was also significantly upregulated in MSC^{GATA-4} than in MSC^{Null} (Fig. 8) ($p < 0.05$). However, no significant differences in the Kv4.2 channel mRNA could be observed between both groups (Fig. 8B) ($p > 0.05$). These results provide potential molecular regulators of the functional ionic currents (i.e., $I_{Na.TTX}$, $I_{Ca.L}$, I_{to}, I_{K1} and I_{KDR}) which were increased in MSC^{GATA-4}.

3.12. Effect of bFGF, VEGF and IGF-1 on ion channel subunits

We further show that MSC^{GATA-4} treated with neutralizing antibodies to IGF-1 display a significant reduction in Kv2.1 channel mRNA expression, compared with untreated MSC^{GATA-4} (IGF-1 treated MSC^{GATA-4}: 53.1 ± 2.1% versus untreated MSC^{GATA-4}: 68.5 ± 5.2%, $p < 0.05$) (Fig. 8A). A significant reduction in Kir1.1, Kv1.4, CCHL2a and SCN2a1 channel mRNA expression was also observed in treated MSC^{GATA-4} (Kir1.1: 30.5 ± 2.7%, Kv1.4: 40.1 ± 3.4%, CCHL2a: 32.2 ± 2.1% and SCN2a1: 42.1 ± 3.1%), compared with untreated MSC^{GATA-4} (Kir1.1: 44.8 ± 4.2%, Kv1.4: 56.1 ± 5.1%, CCHL2a: 41.2 ± 4.1%, SCN2a1: 54.4 ± 5.2%) (Fig. 8) ($p < 0.05$). However, no significant effects of IGF-1 neutralizing antibodies were observed on the expression of Kv1.2 and Kv4.2 mRNA expression in treated versus untreated MSC^{GATA-4} (Fig. 8A).

VEGF neutralizing antibodies had similar effects on mRNA expression levels of these ion channels in MSC^{GATA-4}. Specifically, Kv2.1, Kv1.2, Kv1.4, Kir1.1, CCHL2a and SCN2a1 channel mRNA expression was significantly decreased in MSC^{GATA-4} treated with VEGF neutralizing antibodies (Kv2.1: 51.2 ± 3.1%, Kv1.2: 42.1 ± 3.1%, Kv1.4: 38.1 ± 3.1%, Kir1.1: 29.2 ± 2.9%, CCHL2a: 30.1 ± 2.3%, SCN2a1: 40.2 ± 3.1%), compared with untreated MSC^{GATA-4} (Kv2.1: 68.5 ± 5.2%, Kv1.2: 53.5 ± 6.1%, Kv1.4: 56.1 ± 5.1%, Kir1.1: 44.8 ± 4.2%, CCHL2a: 41.2 ± 4.1%, SCN2a1: 54.4 ± 5.2%) (Fig. 8) ($p < 0.05$). However, VEGF did not significantly alter the expression of Kv4.2 mRNA in treated versus untreated MSC^{GATA-4} (Fig. 8A).

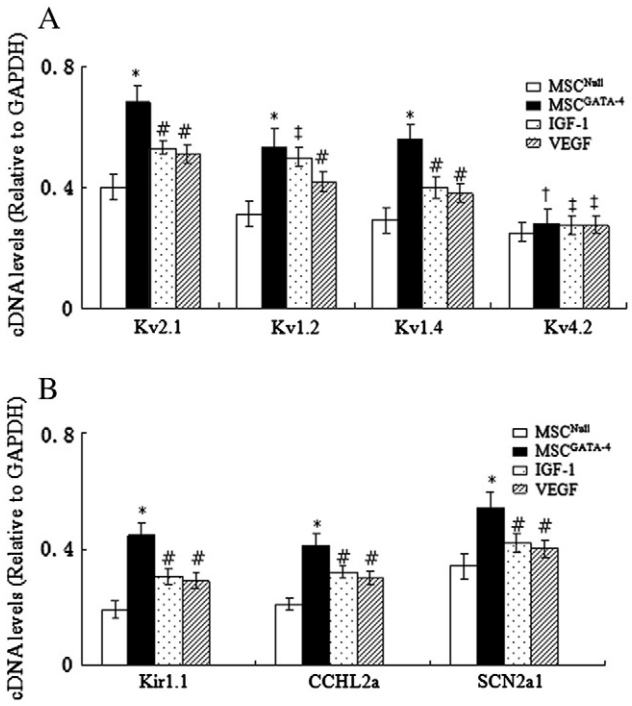

Fig. 8. Real-time PCR analysis of mRNA levels of ion channel subunits associated with functional ionic currents. Summary of amplification of cDNAs derived from MSC mRNAs (n = 5; times of real-time PCR experiments from different cells as used in ion channel study) relative to the housekeeping gene, GAPDH. (A) $K_V1.2$, $K_V2.1$, $K_V1.4$ and $K_V4.2$ mRNA expression levels in MSC. (B) Kir1.1, CCHL2a and SCN2a1 channel mRNA expression levels in MSC. $^{*}p < 0.05$ vs MSC^{Null}. $^{\#}p < 0.05$ vs MSC^{GATA-4}. $^{\dagger}p > 0.05$ vs MSC^{Null} and $^{\ddagger}p > 0.05$ vs MSC^{GATA-4}, n = 5. Abbreviations: CCHL2a, L-type calcium channel α-2 subunit; GAPDH, glyceraldehyde-3-phosphate dehydrogenase; Kir, inward rectifier potassium channel; Kv, voltage-gated potassium channel.

4. Discussion

A major finding of our study is that GATA-4 increases functional ionic currents (i.e., I_{to}, I_{KDR}, I_{K1}, $I_{Na.TTX}$ and $I_{Ca.L}$) in MSC, concomitant with an upregulation in mRNA expression of molecular regulators of these ion channels (i.e., Kv1.4, Kv1.2 and Kv2.1, Kir1.1, SCN2a1 and CCHL2a, respectively), which are found in CM. The functional validity of these ion channels was assessed with the use of inhibitors such as $BaCl_2$ which inhibits I_{k1}, TEA which inhibits IK_{DR}, TTX which blocks

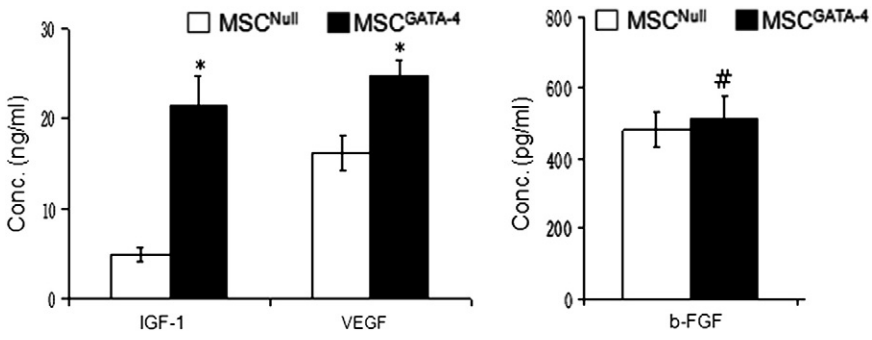

Fig. 7. ELISA analysis of VEGF, IGF-1, and bFGF levels in culture media of transduced MSC. $^{*}p < 0.05$ vs MSC^{Null} and $^{\#}p > 0.05$ vs MSC^{Null}, n = 5.

$I_{Na.TTX}$, 4-AP which blocks I_{to} and nifedipine which inhibits $I_{Ca.L}$. We also demonstrated that the effects of GATA-4 overexpression on upregulation of ionic currents in MSC is at least partially dependent on secreted IGF-1, which in turn could upregulate Kv2.1, Kv1.4, Kir1.1, CCHL2a and SCN2a1 channel transcript levels. In addition, these effects are also partially dependent on secreted VEGF, which in turn can also upregulate Kv2.1, Kv1.2, Kv1.4, Kir1.1, CCHL2a and SCN2a1 channel transcript levels. To our knowledge, this study is the first to demonstrate that genetic modification of MSC via GATA-4 overexpression can directly activate ionic currents specifically found in CM, which could be a possible mechanism of how GATA-4 promotes differentiation of MSC into CM.

4.1. Electrophysiological properties of MSC^{GATA-4}

MSC transplantation can help improve the cardiac function of injured hearts through regeneration of CM [24]. GATA-4 gene enhancement in donor cells has been shown to decrease cell apoptosis, promote angiogenesis and improve differentiation of cells into CM. Specific to differentiation, it has been reported that upregulation of GATA-4 can significantly increase differentiation of P19 (a murine embryonic carcinoma cell line) cells, embryonic stem cells and cardiac stem cells into CM [25,26]. A recent report indicates that SUR2A, a regulatory subunit of cardiac KATP channels, affects GATA-4 expression and shifts CM to less differentiated states [27]. This phenomenon indicates that reduced levels of GATA-4 may even suppress CM differentiation. Our previous research demonstrated that overexpression of GATA-4 can also significantly increase MSC differentiation into CM, which was associated with an upregulation of IGFBP-4 [16]. However, the characterization of the effects of GATA-4 overexpression on differentiation of MSC into CM was limited to assessing CM-specific markers using immunofluorescence microscopy, Western blot and real-time PCR analyses. Immunostaining analyses showed that co-cultured MSC^{GATA-4} were positive for α-sarcomeric actinin. Additionally, real-time PCR and Western blot analyses demonstrated that overexpression of GATA-4 can enhance CM-specific markers such as, BNP, islet-1 and α-actinin when MSC are cultured alone and when they are co-cultured with CM. However, the impact of differentiation factors on the electrophysiological properties and expression patterns of ion channels in MSC has not been well-documented.

Through our studies, we show that GATA-4 expressing MSC co-cultured with CM exhibited I_{K1}, I_{to}, $I_{Na.TTX}$ and $I_{Ca.L}$ channel activities that are all ionic channels typical of CM. Specifically, we demonstrated that MSC^{GATA-4} exhibited larger I_{to} currents than MSC^{Null}, suggesting that GATA-4 induces an increase in I_{to}. As a result, the transcript levels of Kv4.2 and Kv1.4, which encode the α-subunit of I_{to} channel, were further investigated. We show that Kv1.4 but not Kv4.2 transcripts were increased in MSC^{GATA-4} compared to MSC^{Null}. I_{K1} was also increased in MSC^{GATA4} when compared to MSC^{Null}, which might contribute to the observed higher levels of Kir1.1 mRNA in MSC^{GATA4}. In addition, I_{Na} was also increased in MSC^{GATA4} when compared to MSC^{Null}, which could contribute to the observed higher levels of SCN2a1 mRNA in MSC^{GATA4}. I_{Ca-L} was also significantly increased in MSC^{GATA4} when compared to MSC^{Null}, which might also contribute to the higher expression of CCHL2a mRNA. I_{KDR} was also significantly increased in MSC^{GATA4} when compared to MSC^{Null}, which may contribute to the higher expression of Kv2.1 and Kv1.2 mRNAs. Our studies extend previous observations, which demonstrated that newly formed MSC formed by co-culturing MSC with CM (ratio of 1:10) exhibit I_{K1} activity that is an ionic channel typical of CM [28].

4.2. Cytokine mediated electrophysiological changes in MSC expressing GATA-4

Previously, it has been shown that MSC can differentiate into CM-like cells in a myocardial environment without making physical contacts with myocytes [28]. It is well known that MSC secrete a wide array of cytokines such as stem-cell factor (SCF), tumor necrosis factor (TNF), VEGF, IGF-1 and bFGF [29]. Among them, bFGF and IGF-1 are released at higher levels and have been shown to be essential for cellular proliferation and differentiation during heart development [30,31]. Both bFGF and IGF-1 have also been shown to regulate potassium channel expression [32–36]. Previous studies showed that IGF-1 and VEGF are specifically elevated in culture media of MSC co-cultured with CM, suggesting an association with increased CM survival using co-culturing methods [26,37]. Gamper N et al. also reported that IGF-1 upregulates Kv1.1, Kv1.2 and Kv1.3 mRNA in HEK293 cells through PI3-kinase, PDK1 and SGK1 signaling pathways [35]. In cultured neonatal rat ventricular CM, IGF-1 has also been shown to increase cardiac Kv1.5 channel expression by calmodulin-dependent kinase and tyrosine kinase signaling pathways [36]. Previous studies demonstrated that bFGF increases I_{to} in MSC through the upregulation of Kv4.2 expression, but not Kv4.3 [38]. These results altogether suggest a relationship between cytokines and electrophysiological properties of cardiac cells.

Through our studies, we show that VEGF upregulates the expression of Kv2.1, Kv1.2, Kv1.4, Kir1.1, CCHL2a and SCN2a1 channel transcripts, whereas IGF-1 upregulates the expression of Kv2.1, Kv1.4, Kir1.1, CCHL2a and SCN2a1 channel transcript levels in MSC after GATA-4 expression. These results altogether suggest that MSC expressing GATA-4 exert their effects on I_{to}, at least in part, through releasing VEGF or/and IGF-1, which regulates the expression of Kv1.4 channel and increases I_{to} densities in MSC. In terms of the effects of GATA-4 expression on IK_{DR} in MSC, our results suggest that they are primarily mediated through releasing IGF-1, which regulate the expression of the Kv2.1 channel. In terms of the effects of GATA-4 expression on I_{K1}, $I_{Ca.L}$ and $I_{Na.TTX}$ in MSC, our results suggest that they are mediated through release of VGEF and IGF-1, which then regulate the expression of Kir1.1, CCHL2a and SCN2a1 channel transcripts, respectively. In contrast, our results show that GATA-4 expression did not affect the expression of Kv4.2 mRNA.

In conclusion, we identify that there is an impact of GATA-4 expression on the cellular electrophysiological changes in MSC, which include effects on potassium, calcium and sodium channels. However, further experiments are needed to elucidate the underlying mechanisms of how cytokines secreted from MSC^{GATA-4} upregulate the gene expression pattern of ion channels. Future studies aimed at studying these mechanisms will be investigated.

5. Conclusions

GATA-4 overexpression increases I_{to}, IK_{DR}, I_{K1}, $I_{Na.TTX}$ and $I_{Ca.L}$ currents in MSC. Cytokine (VGEF and IGF-1) release from GATA-4 overexpressing MSC can partially account for the upregulated ion channel mRNA expression.

Acknowledgements

This work was supported by a grant-in-aid from the Jiangsu Province for Graduate Research and Innovative Projects in China (Grant No. CXZZ11_0118), the National Natural Scientific Fund Committee in China (Grant Nos. 81100173, 81070139, 81170174 and 81170173), and the Jiangsu Province's Innovation of Medical Team and Leading Talents (Grant No. LJ201140).

References

[1] Y. Miyahara, N. Nagaya, M. Kataoka, B. Yanagawa, K. Tanaka, H. Hao, K. Ishino, H. Ishida, T. Shimizu, K. Kangawa, S. Sano, T. Okano, S. Kitamura, H. Mori, Monolayered mesenchymal stem cells repair scarred myocardium after myocardial infarction, Nat. Med. 12 (2006) 459–465.
[2] B.E. Strauer, M. Brehm, T. Zeus, M. Kostering, A. Hernandez, R.V. Sorg, G. Kogler, P. Wernet, Repair of infarcted myocardium by autologous intracoronary mononuclear bone marrow cell transplantation in humans, Circulation 106 (2002) 1913–1918.

[3] L. Li, S. Zhang, Y. Zhang, B. Yu, Y. Xu, Z. Guan, Paracrine action mediate the antifibrotic effect of transplanted mesenchymal stem cells in a rat model of global heart failure, Mol. Biol. Rep. 36 (2009) 725–731.
[4] H.C. Quevedo, K.E. Hatzistergos, B.N. Oskouei, G.S. Feigenbaum, J.E. Rodriguez, D. Valdes, P.M. Pattany, J.P. Zambrano, Q. Hu, I. McNiece, A.W. Heldman, J.M. Hare, Allogeneic mesenchymal stem cells restore cardiac function in chronic ischemic cardiomyopathy via trilineage differentiating capacity, Proc. Natl. Acad. Sci. U. S. A. 106 (2009) 14022–14027.
[5] H. Kawada, J. Fujita, K. Kinjo, Y. Matsuzaki, M. Tsuma, H. Miyatake, Y. Muguruma, K. Tsuboi, Y. Itabashi, Y. Ikeda, S. Ogawa, H. Okano, T. Hotta, K. Ando, K. Fukuda, Nonhematopoietic mesenchymal stem cells can be mobilized and differentiate into cardiomyocytes after myocardial infarction, Blood 104 (2004) 3581–3587.
[6] M. Rota, J. Kajstura, T. Hosoda, C. Bearzi, S. Vitale, G. Esposito, G. Iaffaldano, M.E. Padin-Iruegas, A. Gonzalez, R. Rizzi, N. Small, J. Muraski, R. Alvarez, X. Chen, K. Urbanek, R. Bolli, S.R. Houser, A. Leri, M.A. Sussman, P. Anversa, Bone marrow cells adopt the cardiomyogenic fate in vivo, Proc. Natl. Acad. Sci. U. S. A. 104 (2007) 17783–17788.
[7] J.S. Burchfield, S. Dimmeler, Role of paracrine factors in stem and progenitor cell mediated cardiac repair and tissue fibrosis, Fibrogenesis & Tissue Repair 1 (2008) 4.
[8] J. Cho, P. Zhai, Y. Maejima, J. Sadoshima, Myocardial injection with GSK-3beta-overexpressing bone marrow-derived mesenchymal stem cells attenuates cardiac dysfunction after myocardial infarction, Circ. Res. 108 (2011) 478–489.
[9] S.H. Kim, H.H. Moon, H.A. Kim, K.C. Hwang, M. Lee, D. Choi, Hypoxia-inducible vascular endothelial growth factor-engineered mesenchymal stem cells prevent myocardial ischemic injury, Mol. Ther. 19 (2011) 741–750.
[10] S. Pikkarainen, H. Tokola, R. Kerkela, H. Ruskoaho, GATA transcription factors in the developing and adult heart, Cardiovasc. Res. 63 (2004) 196–207.
[11] M. Xu, R.W. Millard, M. Ashraf, Role of GATA-4 in differentiation and survival of bone marrow mesenchymal stem cells, Prog. Mol. Biol. Transl. Sci. 111 (2012) 217–241.
[12] J. Rysa, O. Tenhunen, R. Serpi, Y. Soini, M. Nemer, H. Leskinen, H. Ruskoaho, GATA-4 is an angiogenic survival factor of the infarcted heart, Circ. Heart Fail. 3 (2010) 440–450.
[13] H. Li, S. Zuo, Z. He, Y. Yang, Z. Pasha, Y. Wang, M. Xu, Paracrine factors released by GATA-4 overexpressed mesenchymal stem cells increase angiogenesis and cell survival, Am. J. Physiol. Heart Circ. Physiol. 299 (2010) H1772–H1781.
[14] B. Yu, M. Gong, Y. Wang, R.W. Millard, Z. Pasha, Y. Yang, M. Ashraf, M. Xu, Cardiomyocyte protection by GATA-4 gene engineered mesenchymal stem cells is partially mediated by translocation of miR-221 in microvesicles, PloS One 8 (2013) e73304.
[15] C. Grepin, G. Nemer, M. Nemer, Enhanced cardiogenesis in embryonic stem cells overexpressing the GATA-4 transcription factor, Development 124 (1997) 2387–2395.
[16] H. Li, S. Zuo, Z. Pasha, B. Yu, Z. He, Y. Wang, X. Yang, M. Ashraf, M. Xu, GATA-4 promotes myocardial transdifferentiation of mesenchymal stromal cells via up-regulating IGFBP-4, Cytotherapy 13 (2011) 1057–1065.
[17] A.S. Dhamoon, J. Jalife, The inward rectifier current (IK1) controls cardiac excitability and is involved in arrhythmogenesis, Heart Rhythm 2 (2005) 316–324.
[18] R. Sah, R.J. Ramirez, G.Y. Oudit, D. Gidrewicz, M.G. Trivieri, C. Zobel, P.H. Backx, Regulation of cardiac excitation–contraction coupling by action potential repolarization: role of the transient outward potassium current (I(to)), J. Physiol. 546 (2003) 5–18.
[19] D.R. Scriven, E.D. Moore, Ca(2)(+) channel and Na(+)/Ca(2)(+) exchange localization in cardiac myocytes, J. Mol. Cell. Cardiol. 58 (2013) 22–31.
[20] C.A. Remme, C.R. Bezzina, Sodium channel (dys)function and cardiac arrhythmias, Cardiovasc. Ther. 28 (2010) 287–294.
[21] C.A. Ward, H. Bazzazi, R.B. Clark, A. Nygren, W.R. Giles, Actions of emigrated neutrophils on Na(+) and K(+) currents in rat ventricular myocytes, Prog. Biophys. Mol. Biol. 90 (2006) 249–269.
[22] G.R. Li, X.L. Deng, H. Sun, S.S. Chung, H.F. Tse, C.P. Lau, Ion channels in mesenchymal stem cells from rat bone marrow, Stem Cells 24 (2006) 1519–1528.
[23] H.X. Li, R.X. Wang, X.R. Li, T. Guo, Y. Wu, S.X. Guo, L.P. Sun, Z.Y. Yang, X.J. Yang, W.P. Jiang, Increasing DHA and EPA concentrations prolong action potential durations and reduce transient outward potassium currents in rat ventricular myocytes, Lipids 46 (2011) 163–170.
[24] H. Tsuji, S. Miyoshi, Y. Ikegami, N. Hida, H. Asada, I. Togashi, J. Suzuki, M. Satake, H. Nakamizo, M. Tanaka, T. Mori, K. Segawa, N. Nishiyama, J. Inoue, H. Makino, K. Miyado, S. Ogawa, Y. Yoshimura, A. Umezawa, Xenografted human amniotic membrane-derived mesenchymal stem cells are immunologically tolerated and transdifferentiated into cardiomyocytes, Circ. Res. 106 (2010) 1613–1623.
[25] D.L. Hu, F.K. Chen, Y.Q. Liu, Y.H. Sheng, R. Yang, X.Q. Kong, K.J. Cao, H.T. Gu, L.M. Qian, GATA-4 promotes the differentiation of P19 cells into cardiac myocytes, Int. J. Mol. Med. 26 (2010) 365–372.
[26] S. Miyamoto, N. Kawaguchi, G.M. Ellison, R. Matsuoka, T. Shin'oka, H. Kurosawa, Characterization of long-term cultured c-kit + cardiac stem cells derived from adult rat hearts, Stem Cells Dev. 19 (2010) 105–116.
[27] S.C. Land, D.J. Walker, Q. Du, A. Jovanovic, Cardioprotective SUR2A promotes stem cell properties of cardiomyocytes, Int. J. Cardiol. 168 (2013) 5090–5092.
[28] X. Li, X. Yu, Q. Lin, C. Deng, Z. Shan, M. Yang, S. Lin, Bone marrow mesenchymal stem cells differentiate into functional cardiac phenotypes by cardiac microenvironment, J. Mol. Cell. Cardiol. 42 (2007) 295–303.
[29] R. Uemura, M. Xu, N. Ahmad, M. Ashraf, Bone marrow stem cells prevent left ventricular remodeling of ischemic heart through paracrine signaling, Circ. Res. 98 (2006) 1414–1421.
[30] A.W. Li, G. Seyoum, R.P. Shiu, P.R. Murphy, Expression of the rat BFGF antisense RNA transcript is tissue-specific and developmentally regulated, Mol. Cell. Endocrinol. 118 (1996) 113–123.
[31] H. Ulger, A.K. Karabulut, M.K. Pratten, The growth promoting effects of bFGF, PD-ECGF and VEGF on cultured postimplantation rat embryos deprived of serum fractions, J. Anat. 197 (Pt 2) (2000) 207–219.
[32] W. Guo, K. Kamiya, J. Toyama, bFGF promotes functional expression of transient outward currents in cultured neonatal rat ventricular cells, Pflugers Arch. 430 (1995) 1015–1017.
[33] W. Guo, K. Kamiya, J. Toyama, Modulated expression of transient outward current in cultured neonatal rat ventricular myocytes: comparison with development in situ, Cardiovasc. Res. 32 (1996) 524–533.
[34] W. Scharbrodt, C.R. Kuhlmann, Y. Wu, C.A. Schaefer, A.K. Most, U. Backenkohler, T. Neumann, H. Tillmanns, B. Waldecker, A. Erdogan, J. Wiecha, Basic fibroblast growth factor-induced endothelial proliferation and NO synthesis involves inward rectifier K^+ current, Arterioscler. Thromb. Vasc. Biol. 24 (2004) 1229–1233.
[35] N. Gamper, S. Fillon, S.M. Huber, Y. Feng, T. Kobayashi, P. Cohen, F. Lang, IGF-1 up-regulates K^+ channels via PI3-kinase, PDK1 and SGK1, Pflugers Arch. 443 (2002) 625–634.
[36] W. Guo, K. Kamiya, K. Yasui, I. Kodama, J. Toyama, Alpha1-adrenoceptor agonists and IGF-1, myocardial hypertrophic factors, regulate the Kv1.5 K^+ channel expression differentially in cultured newborn rat ventricular cells, Pflugers Arch. 436 (1998) 26–32.
[37] S. Sadat, S. Gehmert, Y.H. Song, Y. Yen, X. Bai, S. Gaiser, H. Klein, E. Alt, The cardioprotective effect of mesenchymal stem cells is mediated by IGF-I and VEGF, Biochem. Biophys. Res. Commun. 363 (2007) 674–679.
[38] C. Benzhi, Z. Limei, W. Ning, L. Jiaqi, Z. Songling, M. Fanyu, Z. Hongyu, L. Yanjie, A. Jing, Y. Baofeng, Bone marrow mesenchymal stem cells upregulate transient outward potassium currents in postnatal rat ventricular myocytes, J. Mol. Cell. Cardiol. 47 (2009) 41–48.